Eur. Phys. J. C 54, 451–460 (2008)
DOI 10.1140/epjc/s10052-008-0531-8

THE EUROPEAN PHYSICAL JOURNAL C

Regular Article – Theoretical Physics

One-loop corrections to the Drell–Yan process in SANC

(II) The neutral current case

A. Arbuzov[1,2], D. Bardin[2], S. Bondarenko[1,2,a], P. Christova[2], L. Kalinovskaya[2], G. Nanava[3,b], R. Sadykov[2]

[1] Bogoliubov Laboratory of Theoretical Physics, JINR, Dubna, 141980 Russia
[2] Dzhelepov Laboratory of Nuclear Problems, JINR, Dubna, 141980 Russia
[3] IFJ, PAN, Krakow, 313-42 Poland

Received: 9 November 2007 /
Published online: 14 February 2008 –

Abstract. Radiative corrections to the neutral current Drell–Yan-like processes are considered. Complete one-loop electroweak corrections are calculated within the SANC system. Theoretical uncertainties are discussed. Numerical results are presented for typical conditions of LHC experiments.

PACS. 13.85.Qk; 12.15.Lk

1 Introduction

The current theoretical status of Drell–Yan [1] physics is widely overviewed in [2,3], where the necessity of further in-depth study of the Drell–Yan-like (DY) processes is emphasized.

At hadron–hadron colliders DY processes serve normalization purposes [4,5], provide information about weak interactions [6,7], and contribute to the background in many searches for new physics beyond the standard model (SM). At the LHC they will be used also for precision fits of partonic density functions in the regions of x and factorization scale values that were not yet accessed experimentally.

The theoretical calculations of the DY processes for high energy hadronic colliders were performed at the level of one-loop QED and electroweak (EW) radiative corrections (RC) by several groups; see [8–17] and references therein. QCD corrections are known up to the next-to-next-to-leading order [18–20].

For the experiment, both charge current (CC) and neutral current (NC) DY processes are of great interest. Both types of processes can easily be detected. CC processes have a larger cross section, but NC processes have a clean dimuon signature and provide additional information, e.g., about the weak mixing angle.

The theoretical study for CC DY is pushed ahead more than for NC – several independent codes exist for EW NLO RC [3]. Within the 2005 Les Houches workshop [21] and the 2006 TEV4LHC workshop [22] a tuned comparison at partonic and hadronic levels at one-loop precision was realized between four codes: [12], [15], [16] and [23–25].

To the contrary, a detailed tuned comparison for neutral current DY NLO either at parton or at hadron levels is still underway. In [26] one can find a comparison between the results of the HORACE and ZGRADE codes for the inclusive NC DY cross section at the hadronic level. Partial results of the comparison at the partonic level between SANC and another code can be found in [27].

This article is the second step in a series of SANC papers devoted to DY processes. First, we presented in [28,29] the CC case. Here we show results for the NC case. Moreover, in the DY branches of SANC we can study the interplay between QCD and EW NLO corrections within the same framework. The current status of this study was presented in the report to the ATLAS MC working group at CERN [30]. A detailed description of the QCD branch for DY CC and NC processes will be presented elsewhere, though the first results are already published in [31].

The paper is organized as follows. In the second section we demonstrate the implementation of the EW NLO corrections into the SANC framework [23,24]. The location of the standard set of the SANC modules, **FF** (form factors), **HA** (helicity amplitudes), **BR** and **MC** (bremsstrahlung), is shown on the screenshot of the **SANC Processes** in the **EW 4f NC** sector. Ibidem we show the rather short analytical expression for the differential cross section of the hard photon contribution.

The SANC team has the advantage of experience in the calculation of bremsstrahlung. We can obtain the numerical results both by the semi-analytical expressions (it is the standard **BR** module of the SANC) and by a Monte Carlo integrator or generator (with the help of the new **MC** module).

[a] e-mail: bondarenko@jinr.ru, sanc@jinr.ru
[b] on leave from IHEP, TSU, Tbilisi, Georgia

In the third section we describe the adopted "subtraction" procedure in the expressions for virtual, soft and hard contributions to the NC DY cross section.

Numerical results are presented in Sect. 4 both for the Born and for the EW NLO RC. We investigated the independence of the result on the variation of the soft–hard separator $\bar{\omega}$, which provides one of the most important checks of the calculation. The sensitivity of the corrections to the variation of "subtracted" quark mass singularities was also studied.

In the conclusion we overview the present status of the implementation of NC DY calculations into the SANC system.

As the main point of this article we offer for the import a stand-alone code for NC DY EW NLO RC at the partonic level together with the environment in which it was run. A sketchy description of this code is presented in the appendix.

For the production of numbers at the hadronic level the SANC team created a Monte Carlo integrator and an event generator, based on the FOAM package [32]. The generator itself will be described elsewhere [33].

The package for the calculations at the partonic level and the generator based on the FOAM mentioned above are accessible from the SANC project homepages [34, 35].

2 Neutral current Drell–Yan processes

2.1 Born level

At first we will consider interactions of *free* quarks (partons). At the leading order (LO) the unpolarized cross section of the partonic subprocess $\bar{q}(p_1)+q(p_2)\to(\gamma,Z)\to \ell(p_3)+\bar{\ell}(p_4)$, $q=(u,d,c,s,b)$ is given by

$$\hat{\sigma}_0(\hat{s})=\frac{4\pi\alpha^2}{9\hat{s}}\beta_{\hat{s}}\left[\left(1-\frac{m_\ell^2}{\hat{s}}\right)V_0(\hat{s})+\frac{3m_\ell^2}{\hat{s}}V_A(\hat{s})\right], \quad (1)$$

where

$$\hat{s}=-(p_1+p_2)^2,$$
$$\beta_{\hat{s}}=\sqrt{1-\frac{4m_\ell^2}{\hat{s}}}\,, \quad (2)$$

and m_ℓ being the lepton mass. Here we denoted

$$\begin{aligned} V_{0,A}(\hat{s}) &= Q_q^2Q_\ell^2+2Q_qQ_\ell v_qv_\ell \mathrm{Re}\chi(\hat{s}) \\ &\quad +\left(v_q^2+a_q^2\right)\left(v_\ell^2\pm a_\ell^2\right)\mid\chi(\hat{s})\mid^2, \\ v_q &= I_q^{(3)}-2Q_q\sin^2\theta_\mathrm{W}, \\ v_\ell &= I_\ell^{(3)}-2Q_\ell\sin^2\theta_\mathrm{W}, \\ a_q &= I_q^{(3)}, \\ a_\ell &= I_\ell^{(3)}. \end{aligned} \quad (3)$$

The Z/γ propagator ratio $\chi_Z(\hat{s})$ with constant (or $\hat{s}$-dependent) Z width reads

$$\chi_Z(\hat{s})=\frac{1}{4s_\mathrm{W}^2c_\mathrm{W}^2}\frac{\hat{s}}{\hat{s}-M_Z^2+\mathrm{i}M_Z\Gamma_Z}, \quad (4)$$

where s_W and c_W are the sine and cosine of the Weinberg weak mixing angle θ_W.

2.2 EW radiative corrections at the partonic level

As the rule of the SANC basement, we subdivide the EW RC into the virtual (loop) ones, the ones due to soft photon emission, and the ones due to hard photon emission. Later on in Sect. 4 in Tables 1 and 2, we demonstrate the independence of the EW RC of an auxiliary parameter $\bar{\omega}$ that subdivides the soft and hard photonic contributions.

In Fig. 1 we show the location of the $2f\to 2f$ NC processes at the SANC tree.

Moving along the menu sequence **SANC** → **EW** → **Processes** → **4 legs** → **4f** → **Neutral Current** → **f1 f1** → **f f** (**FF,HA,BR,MC**) the user arrives at the first standard SANC module, the scalar form factors (FF); then at the second module, the helicity amplitudes (HA); then at the third module, the integrated bremsstrahlung (BR); and finally at the fourth module, the fully differential bremsstrahlung (MC).

• FF and HA.

In [23, 24] we presented the covariant (CA) and helicity amplitudes (HA) of the $f_1\bar{f}_1f\bar{f}\to 0$ NC process, with all 4-momenta being incoming, for any of its cross channels s,t or u. The expressions for the CA and HA (see (30) and (33) of the latter reference) of this process can be written in terms of six FF.

• BR and MC.

The BR module computes the soft and inclusive hard real photon emission:

$$\bar{q}(p_1)+q(p_2)\to\ell(p_3)+\bar{\ell}(p_4)+\gamma(p_5), \quad (5)$$

where the momenta of the corresponding particles are given in brackets. We do not discuss the soft photon contribution here, referring the reader to the system itself. As far as hard photons are concerned, we realized two possibilities of the integration over its phase space: the semi-analytical one (BR) and the one by means of a Monte Carlo integrator or generator (MC).

The first one is based on two different sets of analytical integrals over two choices of kinematic variables parametrizing the hard photon phase space. In the first option (CalcScheme = 0), the phase space looks like

$$\mathrm{d}\Phi^{(3)}=\mathrm{d}\Phi_1^{(2)}\,\mathrm{d}\Phi_2^{(2)}\frac{\mathrm{d}\hat{s}'}{2\pi}, \quad (6)$$

where the two-body phase spaces are

$$\begin{aligned} \mathrm{d}\Phi_1^{(1)} &= \frac{1}{8\pi}\frac{\sqrt{\lambda(\hat{s},\hat{s}',0)}}{\hat{s}}\frac{1}{2}\,\mathrm{d}\cos\theta_\gamma, \\ \mathrm{d}\Phi_2^{(2)} &= \frac{1}{8\pi}\frac{\sqrt{\lambda(\hat{s}',m_\ell^2,m_\ell^2)}}{\hat{s}'}\frac{1}{4\pi}\,\mathrm{d}\cos\theta_3\,\mathrm{d}\phi_3. \end{aligned} \quad (7)$$

Here, $\hat{s}'=-(p_3+p_4)^2$, and θ_γ is the cms angle of the photon. Since for the chosen parametrization of the phase space the matrix element squared of the process does not depend on the angle ϕ_γ – the cms azimuthal angle of the

Table 1. The total lowest-order and one-loop corrected cross sections $\hat{\sigma}_0$ and $\hat{\sigma}_1$ for the process $u\bar{u} \to \mu^+\mu^-(\gamma)$ in the α EW scheme and corresponding relative one-loop correction δ for $\bar{\omega} = 10^{-4}\frac{\sqrt{\hat{s}}}{2}$ GeV, rows 1) and $\bar{\omega} = 10^{-5}\frac{\sqrt{\hat{s}}}{2}$ GeV, rows 2). Cut value: $M_{\mu^+\mu^-} \geq 50$ GeV

$\sqrt{\hat{s}}$, GeV	70	90	110	500	1000	2000	5000	14 000
$\hat{\sigma}_0$, pb	4.312	369.6	4.995	7.324×10^{-2}	1.806×10^{-2}	4.499×10^{-3}	7.191×10^{-4}	9.171×10^{-5}
$\hat{\sigma}_1$, pb	4.713	397.2	4.732	8.403×10^{-2}	2.105×10^{-2}	5.256×10^{-3}	8.269×10^{-4}	1.010×10^{-4}
					$m_q = m_u$			
δ, %, 1)	9.303	7.468	−5.259	14.74	16.61	16.84	14.99	10.09
δ, %, 2)	9.303	7.481	−5.261	14.74	16.61	16.84	14.99	10.09
					$m_q = m_u/10$			
δ, %, 1)	9.296	7.466	−5.261	14.74	16.61	16.84	14.99	10.09
δ, %, 2)	9.296	7.480	−5.263	14.74	16.61	16.84	14.99	10.09

Table 2. The total lowest-order and one-loop corrected cross sections $\hat{\sigma}_0$ and $\hat{\sigma}_1$ for the process $d\bar{d} \to \mu^+\mu^-(\gamma)$ in the α EW scheme and corresponding relative one-loop correction δ for $\bar{\omega} = 10^{-4}\frac{\sqrt{\hat{s}}}{2}$ GeV, rows 1) and $\bar{\omega} = 10^{-5}\frac{\sqrt{\hat{s}}}{2}$ GeV, rows 2). Cut value: $M_{\mu^+\mu^-} \geq 50$ GeV

$\sqrt{\hat{s}}$, GeV	70	90	110	500	1000	2000	5000	14 000
$\hat{\sigma}_0$, pb	2.895	472.9	5.237	3.968×10^{-2}	9.601×10^{-3}	2.381×10^{-3}	3.802×10^{-4}	4.847×10^{-5}
$\hat{\sigma}_1$, pb	3.079	497.3	5.318	4.439×10^{-2}	1.090×10^{-2}	2.692×10^{-3}	4.149×10^{-4}	4.863×10^{-5}
					$m_q = m_d$			
δ, %, 1)	6.328	5.164	1.551	11.88	13.53	13.04	9.142	0.319
δ, %, 2)	6.327	5.167	1.550	11.88	13.53	13.04	9.141	0.317
					$m_q = m_d/10$			
δ, %, 1)	6.329	5.162	1.552	11.88	13.53	13.04	9.142	0.318
δ, %, 2)	6.329	5.165	1.551	11.88	13.53	13.04	9.141	0.317

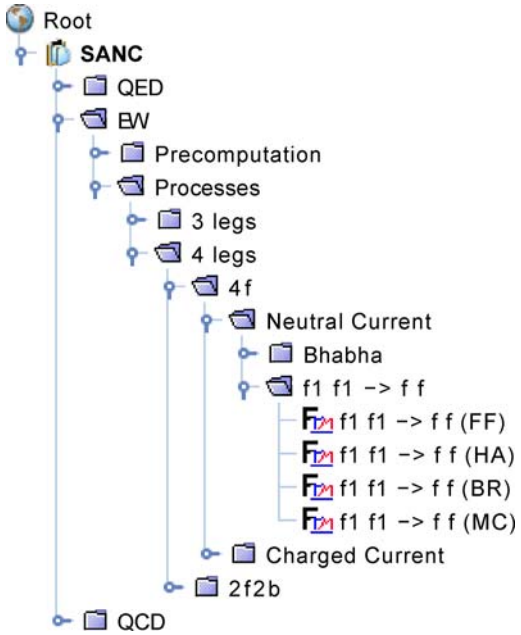

Fig. 1. SANC tree for the process $2f \to 2f$

photon – it is already integrated out in the phase space. The angles θ_3 and ϕ_3 define the orientation of the momentum p_3 in the rest frame of the compound $(p_3 + p_4 = 0)$.

These parameters vary in the limits

$$0 \leq \theta_\gamma, \theta_3 \leq \pi\,, \quad 0 \leq \phi_3 \leq 2\pi\,,$$
$$4m_\ell^2 \leq \hat{s}' \leq \hat{s} - 2\sqrt{\hat{s}}\bar{\omega}\,. \tag{8}$$

After the integration over all angular variables, we obtained the compact expression for a single differential distribution of the hard photon contribution to the NC DY process, $\mathrm{d}\hat{\sigma}_{\mathrm{hard}}/\mathrm{d}\hat{s}'$. We neglected terms proportional to the initial quark mass but kept terms proportional to the lepton mass:

$$\begin{aligned}
\frac{\mathrm{d}\hat{\sigma}_{\mathrm{hard}}}{\mathrm{d}\hat{s}'} = {} & \frac{\alpha}{\pi}\frac{\hat{s}^2+\hat{s}'^2}{\hat{s}^2\hat{s}_-}\left[Q_q^2\left(\ln\frac{\hat{s}}{m_q^2}-1\right)\hat{\sigma}_0(\hat{s}')\right.\\
& \left.+\,Q_\ell^2\left(L'_\beta-\beta_{\hat{s}'}\right)\frac{1}{\beta_{\hat{s}}}\hat{\sigma}_0(\hat{s})\right]+\frac{2\alpha^3}{3}Q_qQ_\ell\frac{\hat{s}_+}{\hat{s}^3}\\
& \times\left[A_2(\hat{s},\hat{s}')\left(\frac{m_\ell^2}{\hat{s}'}\frac{\hat{s}_+}{\hat{s}_-}L'_\beta-\frac{\hat{s}}{\hat{s}_-}\beta_{\hat{s}'}\right)\right.\\
& \left.+\,Q_qQ_\ell A_1(\hat{s},\hat{s}')\frac{m_\ell^2}{\hat{s}'}L'_\beta\right]+\frac{4\alpha^3}{9}Q_\ell^2\frac{m_\ell^2}{\hat{s}^3}\\
& \times\left\{V_0(\hat{s})\left[2\left(\frac{\hat{s}_-}{\hat{s}}-2\frac{\hat{s}-m_\ell^2}{\hat{s}_-}\right)L'_\beta-\frac{\hat{s}_-}{\hat{s}}\beta_{\hat{s}'}\right]\right.\\
& \left.-\,V_A(\hat{s})\left[4\left(\frac{\hat{s}_-}{\hat{s}}+3\frac{m_\ell^2}{\hat{s}_-}\right)L'_\beta-3\frac{\hat{s}_-}{\hat{s}}\beta_{\hat{s}'}\right]\right\},
\end{aligned} \tag{9}$$

where

$$L'_\beta = \ln\frac{1+\beta_{\hat{s}'}}{1-\beta_{\hat{s}'}}\,,$$
$$\hat{s}_\pm = \hat{s} \pm \hat{s}'\,, \tag{10}$$

with the Born cross section given by (1). The coupling functions are

$$A_1(\hat{s},\hat{s}') = 2a_q a_\ell \mathrm{Re}\big[\chi(\hat{s}') - \chi(\hat{s})\big]$$
$$A_2(\hat{s},\hat{s}') = 2Q_q Q_\ell a_q a_\ell \mathrm{Re}\big[\chi(\hat{s}') + \chi(\hat{s})\big] + 8v_q a_q v_\ell a_\ell \mathrm{Re}\big[\chi(\hat{s})\chi^*(\hat{s}')\big]\,. \tag{11}$$

We give also the simpler expression neglecting the lepton masses. Then all masses remain only in the arguments of the logarithms:

$$\frac{\mathrm{d}\hat{\sigma}_{\mathrm{hard}}}{\mathrm{d}\hat{s}'} = \frac{\alpha}{\pi}\frac{1}{\hat{s}_-}\frac{\hat{s}^2+\hat{s}'^2}{\hat{s}^2}\left[Q_q^2\left(\ln\frac{\hat{s}}{m_q^2}-1\right)\hat{\sigma}_0(\hat{s}') + Q_\ell^2\left(\ln\frac{\hat{s}'}{m_\ell^2}-1\right)\hat{\sigma}_0(\hat{s})\right] - \frac{1}{3}\,\frac{\alpha^3}{\hat{s}^2}\frac{\hat{s}_+}{\hat{s}_-}|\,Q_q Q_\ell\,| \times \mathrm{Re}\Big[Q_q Q_\ell\Big(\chi_Z(\hat{s})+\chi_Z(\hat{s}')\Big) + 4\,v_q v_\ell\,\chi_Z(\hat{s})\chi_Z^*(\hat{s}')\Big], \tag{12}$$

with $\hat{\sigma}_0(\hat{s})$ being the massless limit of (1).

In the second option (CalcScheme=1), the module BR computes the distribution: $\mathrm{d}\hat{\sigma}_{\mathrm{hard}}/\mathrm{d}\hat{c}$, where $\hat{c} = \cos(\angle p_2 p_4)$. The phase space in this case reads

$$\mathrm{d}\Phi^{(3)} = \frac{1}{2^9\pi^4\hat{s}}\,\mathrm{d}\hat{c}\,\mathrm{d}\hat{s}'\,\mathrm{d}Z_4\,\mathrm{d}\phi_\gamma\,, \tag{13}$$

where $Z_4 = -2p_4p_5$ and ϕ_γ is the cms azimuthal angle of p_5 varying within 2π limits. After integration over ϕ_γ, Z_4, varying within the limits

$$\frac{1}{2}\hat{s}_-(1-\beta_{\hat{s}}) \le Z_4 \le \frac{1}{2}\hat{s}_-(1+\beta_{\hat{s}}), \tag{14}$$

and $\hat{s}'$ within the same limits as in (8), one gets a very cumbersome result for the single differential distribution over the variable $\hat{c}$, where one has to neglect terms proportional to all masses keeping them only in the arguments of the logarithms. The user may see this result after a corresponding run of the SANC **BR** module with CalcScheme = 1.

The **MC** module provides a fully differential hard bremsstrahlung contribution to the partonic cross section. The contribution is given in a form suitable for further numerical integration or simulation of events in a Monte Carlo generator.

3 Treatment of quark mass singularities

3.1 Partonic level

To perform the subtraction procedure at the partonic level cross section

$$\hat{\sigma}_1 = \hat{\sigma}_0 + \hat{\sigma}_{\mathrm{SV}} + \hat{\sigma}_{\mathrm{hard}}\,, \tag{15}$$

we proceed in the same way as in our previous paper on DY CC [28, 29].

The subtracted expression $\Delta\hat{\sigma}^{\overline{\mathrm{MS}}}$ from the complete calculations with massive quarks becomes

$$\Delta\hat{\sigma}_1^{\overline{\mathrm{MS}}} = \sum_{i=1,2} Q_i^2\frac{\alpha}{2\pi}\int\limits_{\xi_{\min}}^{1}\mathrm{d}\xi_i\left[\frac{1+\xi_i^2}{1-\xi_i}\left(\ln\frac{M^2}{m_i^2} - 2\ln(1-\xi_i) - 1\right)\right]_+\hat{\sigma}_0(s\xi_i)\,, \tag{16}$$

where

$$\xi_{\min} = \frac{4m_\ell^2}{s}\,. \tag{17}$$

Next, Q_i and m_i are the charge and the mass of the given quark; M is the factorization scale; $\hat{\sigma}_0(s\xi_i)$ is the cross section at the partonic level with the reduced value of $s \to s\xi_i$.

The plus prescription in (16) can be treated in the following way:

$$\Delta\hat{\sigma}_1^{\overline{\mathrm{MS}}} = \lim_{\bar{\omega}\to 0}\left(\Delta\hat{\sigma}_{\mathrm{SV}} + \Delta\hat{\sigma}_{\mathrm{hard}}\right)^{\overline{\mathrm{MS}}}. \tag{18}$$

The first contribution, $\Delta\hat{\sigma}_{\mathrm{SV}}$, related to soft and virtual photonic contributions, is given by

$$\Delta\hat{\sigma}_{\mathrm{SV}} = \frac{\alpha}{\pi}Q_q^2\left(\ln\frac{M^2}{m_q^2}\ln\frac{4\bar{\omega}^2}{s} - \frac{1}{2}\ln^2\frac{4\bar{\omega}^2}{s} - \ln\frac{4\bar{\omega}^2}{s} + \frac{3}{2}\ln\frac{M^2}{m_q^2} + 2\right)\hat{\sigma}_0(s)\,, \tag{19}$$

where we took into account that $m_1 = m_2 = m_q$ and $Q_1^2 = Q_2^2 = Q_q^2$ for the NC case.

The second one, $\Delta\hat{\sigma}_{\mathrm{hard}}$, related to hard photon emission, is

$$\Delta\hat{\sigma}_{\mathrm{hard}} = \frac{\alpha}{\pi}Q_q^2\int\limits_{\xi_{\min}}^{\xi_{\max}}\mathrm{d}\xi\left[\frac{1+\xi^2}{1-\xi}\ln\frac{M^2}{m_q^2} - 2\ln(1-\xi) - 1\right]\hat{\sigma}_0(s\xi), \tag{20}$$

where

$$\xi_{\max} = \frac{s-2\sqrt{s}\bar{\omega}}{s}. \tag{21}$$

Using the subtraction procedure, the cross section with $\mathcal{O}(\alpha)$ corrections is given by

$$\hat{\sigma}_1^{\overline{\mathrm{MS}}} = \hat{\sigma}_1 - \Delta\hat{\sigma}_1^{\overline{\mathrm{MS}}}. \tag{22}$$

Then it can be convoluted with PDFs in the usual way. An equivalent subtraction procedure applied at the hadronic level will be discussed right below.

3.2 Hadronic level

The differential cross section of the DY process at the hadronic level can be obtained from the convolution of the partonic cross section with the quark density functions:

$$\frac{\mathrm{d}\sigma_1^{pp\to l\bar{l}X}(s,c)}{\mathrm{d}c} = \sum_{q_1 q_2} \int_0^1 \int_0^1 \mathrm{d}x_1\ \mathrm{d}x_2\ \bar{q}_1(x_1,M^2) \times \bar{q}_2(x_2,M^2) \frac{\mathrm{d}\hat{\sigma}_1^{q_1\bar{q}_2\to l\bar{l}}(\hat{s},\hat{c})}{\mathrm{d}\hat{c}} \mathcal{J}\Theta(c,x_1,x_2)\,, \quad (23)$$

where the step function $\Theta(c,x_1,x_2)$ defines the phase space domain corresponding to the given event selection procedure. The partonic cross section is taken in the center-of-mass reference frame of the initial quarks, where the cosine of the muon scattering angle $\hat{c}$ is defined. The transformation into the angle c defined in the cms of the initial hadrons involves the Jacobian,

$$\mathcal{J} = \frac{\partial\hat{c}}{\partial c} = \frac{4x_1x_2}{a^2}\,, \quad a = x_1+x_2-c(x_1-x_2)\,,$$
$$\hat{c} = 1-(1-c)\frac{2x_1}{a}\,, \qquad \hat{s} = sx_1x_2\,. \quad (24)$$

The parton densities with *bars* in (23) mean the ones modified by subtraction of the quark mass singularities:

$$\bar{q}(x,M^2) = q(x,M^2) - \frac{\alpha}{2\pi}Q_q^2 \int_x^1 \frac{\mathrm{d}z}{z} q\left(\frac{x}{z},M^2\right) \times \left[\frac{1+z^2}{1-z}\left(\ln\frac{M^2}{m_q^2} - 2\ln(1-z) - 1\right)\right]_+\,, \quad (25)$$

where $q(x,M^2)$ can be taken directly from the existing PDFs in the $\overline{\mathrm{MS}}$ scheme (see [10] for the corresponding formula in the DIS scheme). It can be shown analytically that this procedure is equivalent to the subtraction from the cross section, given by (22). In the approach with subtraction from the PDFs it is easy to keep the completely differential form of the subprocess cross section and therefore to impose any kind of experimental cut. When returning to the Z-resonance is allowed by kinematic cuts, the *natural* choice of the factorization scale is $M^2 = M_Z^2$. For the region of higher invariant masses of the lepton pair, $M_{l^+l^-}$, it is better to take $M^2 \sim M_{l^+l^-}^2$.

4 Numerical results

The input parameters set is taken to be the same as used in [21] (`1eshw_input.h`, see the appendix):

$$\begin{array}{ll} G_\mathrm{F} = 1.16637\times10^{-5}\,\mathrm{GeV}^{-2}\,, & \\ \alpha(0) = 1/137.03599911, & \alpha_\mathrm{s} = 0.1187, \\ M_\mathrm{W} = 80.425\,\mathrm{GeV}\,, & \Gamma_W = 2.124\,\mathrm{GeV}\,, \\ M_Z = 91.1867\,\mathrm{GeV}\,, & \Gamma_Z = 2.4952\,\mathrm{GeV}\,, \\ M_H = 150\,\mathrm{GeV}\,, & m_t = 174.17\,\mathrm{GeV}\,, \\ m_e = 0.51099892\times10^{-3}\,\mathrm{GeV}\,, & m_u = m_d = 66\,\mathrm{MeV}\,, \\ m_\mu = 0.105658369\,\mathrm{GeV}\,, & m_c = 1.55\,\mathrm{GeV}\,, \\ m_s = 150\,\mathrm{MeV}\,, & \\ m_\tau = 1.77699\,\mathrm{GeV}\,, & m_b = 4.5\,\mathrm{GeV}\,, \\ |V_{ud}| = |V_{cs}| = 0.975, & |V_{us}| = |V_{cd}| = 0.222. \end{array} \quad (26)$$

4.1 Partonic level

We begin with a presentation of several numerical results derived at the partonic level, investigating the independence of the results of some unphysical parameters and of the choice of the EW scheme. First, we investigate the independence of the parameter $\bar{\omega}$, and the residual dependence on the initial quark masses after the procedure of subtraction of quark mass singularities (see Sect. 3) by choosing for the quark masses two values: first as in (26), and the second ten times lower.

4.1.1 Independence of parameter $\bar{\omega}$ and quark masses

The sum of the "soft" and "hard" photon contributions to the total and differential cross sections should not depend on the soft–hard separator $\bar{\omega}$, which we varied from $10^{-3}\frac{\sqrt{\hat{s}}}{2}$ GeV to $10^{-5}\frac{\sqrt{\hat{s}}}{2}$ GeV. We observed that for $\bar{\omega} = 10^{-4}\frac{\sqrt{\hat{s}}}{2}$ GeV and $\bar{\omega} = 10^{-5}\frac{\sqrt{\hat{s}}}{2}$ GeV the numbers for the one-loop corrected cross sections $\hat{\sigma}_1$ agree within four digits, as shown, and therefore we present only one row in Tables 1 and 2. For the relative radiative correction factors there is a tiny dependence on $\bar{\omega}$, and we present the RC for both $\bar{\omega}$ using the mark 1) for 10^{-4} and 2) for 10^{-5}. The difference between the results for two $\bar{\omega}$ is, however, much below any reasonable estimate of the theoretical accuracy.

The cross sections are shown in picobarn and the radiative corrections in percent. All the results in Tables 1 and 2 are derived in the $\alpha(0)$ EW scheme and *after the subtraction of quark mass singularities in the $\overline{MS}$ scheme*.

Each table contains four rows of δ, two pairs for different $\bar{\omega}$ for $m_u = m_d = 0.066$ GeV and $m_u = m_d = 0.0066$ GeV. After subtraction of quark mass singularities the total cross section should be fully independent of the quark masses. If cuts are applied, a residual dependence arises, in principle, which becomes stronger if the cuts get tighter. The numbers in Tables 1 and 2 are derived for the only cut $M_{\mu^+\mu^-} \geq 50$ GeV. As seen, the residual quark mass dependence is very weak.

All the numbers were obtained with the aid of a FORTRAN code, which consists of a hand-written `main` and FORTRAN modules automatically generated by `s2n.f` software of the SANC system; see the appendix.

4.1.2 $\alpha(0)$, G_F, G'_F schemes

Here we study the EW scheme dependence of the corrected cross section $\hat{\sigma}_1$ arising from the definition of EW constants in the $\alpha(0)$, G_F and G'_F schemes.

In Table 3 we show the results for $\hat{\sigma}_0$ and $\hat{\sigma}_1$ at the Born and one-loop levels and for the corresponding RC factors δ in three EW schemes.

The $\alpha(0)$ and $G_{\rm F}$ EW schemes are defined as usually [36]. In the $G'_{\rm F}$ scheme one assigns the same one-loop value of the coupling constant standing at all photon vertices $\alpha_{\rm QED} \approx 1/132.544$. It has been adopted in [12] and used in [28, 29] for the sake of comparison only.

The results for the radiative corrections are derived in the $\overline{\rm MS}$ subtraction scheme, and the factorization scale is taken to be M_Z. There are notable deviations of the corrected cross sections from the corresponding Born values and between the Born values themselves in the three schemes. One can observe a certain degree of stabilization of one-loop corrected cross sections as can be seen from the rows of Δ values, showing deviations of $\hat{\sigma}_1$ in the $\alpha(0)$ and $G'_{\rm F}$ schemes from $\hat{\sigma}_1$ in the $G_{\rm F}$ scheme:

$$\Delta(\alpha, G'_{\rm F}) = \hat{\sigma}_1(\alpha, G'_{\rm F})/\hat{\sigma}_1(G_{\rm F}) - 1, \% \,. \qquad (27)$$

However, for the process $u\bar{u} \to \mu^+\mu^-(\gamma)$, especially at high energies, the $G'_{\rm F}$ scheme does not seem to work satisfactorily.

Note that for the $\alpha(0)$ scheme it is sufficient to show only the Δ-rows, since all the other entries are already given in Tables 1 and 2.

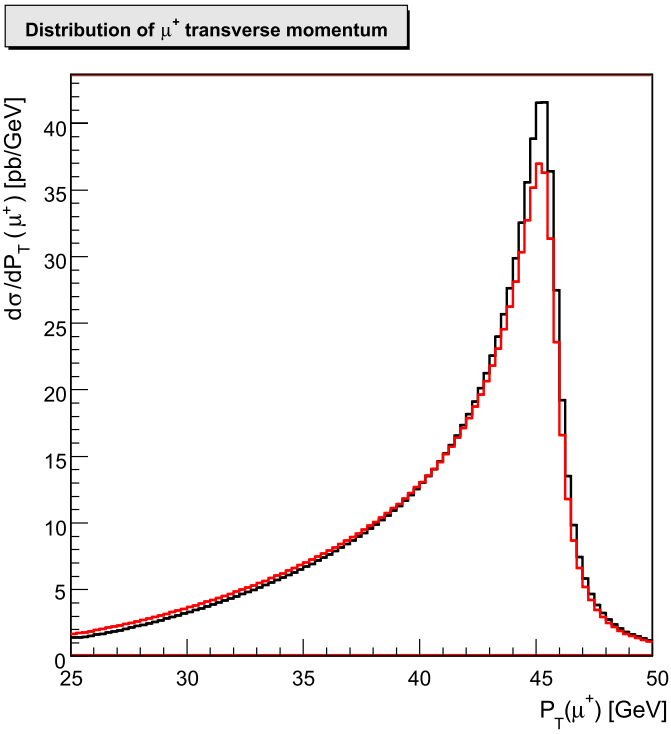

Fig. 2. Muon transverse momentum distribution for $\sqrt{s} = 14\,\text{TeV}$, as obtained from the MC integrator. Both the Born (*upper line*) and the one-loop results (*lower line*) are shown

Table 3. The total lowest-order parton cross section $\hat{\sigma}_0$ and one-loop corrected cross section $\hat{\sigma}_1$ in pb and relative RC factor δ for the two EW schemes $G_{\rm F}$ and $G'_{\rm F}$ for $\bar{\omega} = 10^{-5}\frac{\sqrt{\hat{s}}}{2}$ GeV and invariant mass cut $M_{\mu^+\mu^-} = 50\,\text{GeV}$; for details see the text

$\sqrt{\hat{s}}$, GeV	70	90	110	500	1000	2000	5000	14 000
$u\bar{u} \to \mu^+\mu^-(\gamma)$								
α								
Δ ,%	−0.55	−1.41	−0.34	−0.59	−0.66	−0.64	−0.53	−0.30
$G_{\rm F}$								
$\hat{\sigma}_0$, pb	4.434	394.9	5.259	7.464×10^{-2}	1.839×10^{-2}	4.581×10^{-3}	7.323×10^{-4}	9.338×10^{-5}
$\hat{\sigma}_1$, pb	4.739	402.9	4.748	8.453×10^{-2}	2.119×10^{-2}	5.290×10^{-3}	8.313×10^{-4}	1.013×10^{-4}
δ, %	6.878	2.019	−9.718	13.25	15.23	15.47+	13.53	8.443
$G'_{\rm F}$								
$\hat{\sigma}_0$, pb	4.608	395.0	+5.338	7.826×10^{-2}	1.929×10^{-2}	4.807×10^{-3}	7.685×10^{-4}	9.800×10^{-5}
$\hat{\sigma}_1$, pb	4.805	403.2	4.759	8.657×10^{-2}	2.176×10^{-2}	5.442×10^{-3}	8.576×10^{-3}	1.048×10^{-4}
δ, %	4.285	2.075	−10.83	10.61	12.76	13.21	11.60	6.913
Δ, %	+1.01	+0.07	+0.23	+2.41	+2.69	+2.87	+3.16	+3.46
$d\bar{d} \to \mu^+\mu^-(\gamma)$								
α								
	−0.96	−1.29	−1.02	−1.06	−1.09	−1.07	−0.91	−0.045
$G_{\rm F}$								
$\hat{\sigma}_0$, pb	3.055	505.3	5.573	4.144×10^{-2}	1.002×10^{-2}	2.485×10^{-3}	3.966×10^{-4}	5.057×10^{-5}
$\hat{\sigma}_1$, pb	3.109	503.8	5.373	4.487×10^{-2}	1.102×10^{-2}	2.721×10^{-3}	4.187×10^{-4}	4.885×10^{-5}
δ, %	1.781	−0.306	−3.593	8.268	9.994	9.509	5.550	−3.408
$G'_{\rm F}$								
$\hat{\sigma}_0$, pb	3.094	505.3	5.596	4.240×10^{-2}	1.026×10^{-2}	2.545×10^{-3}	4.062×10^{-4}	5.180×10^{-5}
$\hat{\sigma}_1$, pb	3.126	503.7	5.371	4.534×10^{-2}	1.115×10^{-2}	2.756×10^{-3}	4.240×10^{-4}	4.940×10^{-5}
δ, %	1.026	−0.310	−4.027	6.932	8.718	8.291	4.368	−4.619
Δ, %	+0.55	−0.02	−0.04	+1.05	+1.18	+1.29	1.27	+1.13

Concerning the choice between the $\alpha(0)$ and $G_{\rm F}$ schemes, we favor the latter since its effective energy scale is known to be of the order of a weak boson mass. Moreover, in the results presented in the $\alpha(0)$ scheme, the hadronic contribution to the vacuum polarization in the photon propagator is taken into account in an approximation, using the one-loop formulae supplied by the quark masses listed in (26). In any case the difference between the schemes is related to the contribution of higher orders of the perturbation theory and gives us a crude estimate of the corresponding contribution to the theoretical uncertainty.

4.2 Hadronic level

Results presented in this section were obtained with the aid of two stand-alone packages: 1) a MC integrator based on the Vegas algorithm [37] and 2) a MC generator based on the FOAM algorithm [32]. All the calculations are done with the Les Houches 2005 setup [21] in the $G_{\rm F}$ EW scheme. Besides the input parameters (26), one has to specify cuts on the invariant mass $M_{\mu^+\mu^-}$ of the muons, the transverse momenta $p_{\rm T}(\mu)$ and the pseudo-rapidity $\eta(\mu)$ of the muon, which were used at the production of the figures below:

$$\begin{aligned} &M_{\mu^+\mu^-} > 50\,\text{GeV}\,,\\ &p_{\rm T}(\mu^\pm) > 25\,\text{GeV}\,,\\ &|\eta(\mu^\pm)| < 1.2\,. \end{aligned} \tag{28}$$

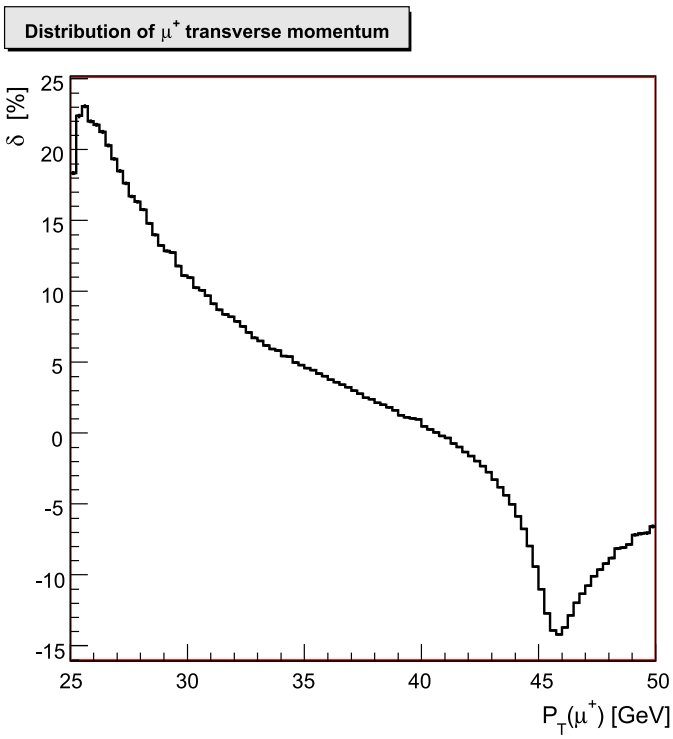

Fig. 3. Relative corrections δ as a function of the muon transverse momentum $p_{\rm T}(\mu^+)$, as obtained from the MC integrator

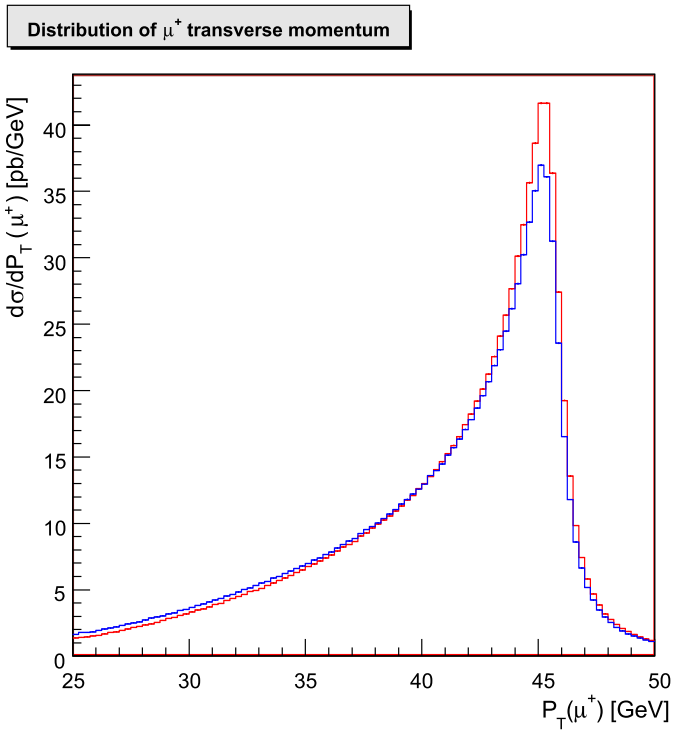

Fig. 4. Muon transverse momentum distribution for $\sqrt{s} = 14\,\text{TeV}$, as obtained from the MC event generator. Both the Born (*upper line*) and the one-loop results (*lower line*) are shown

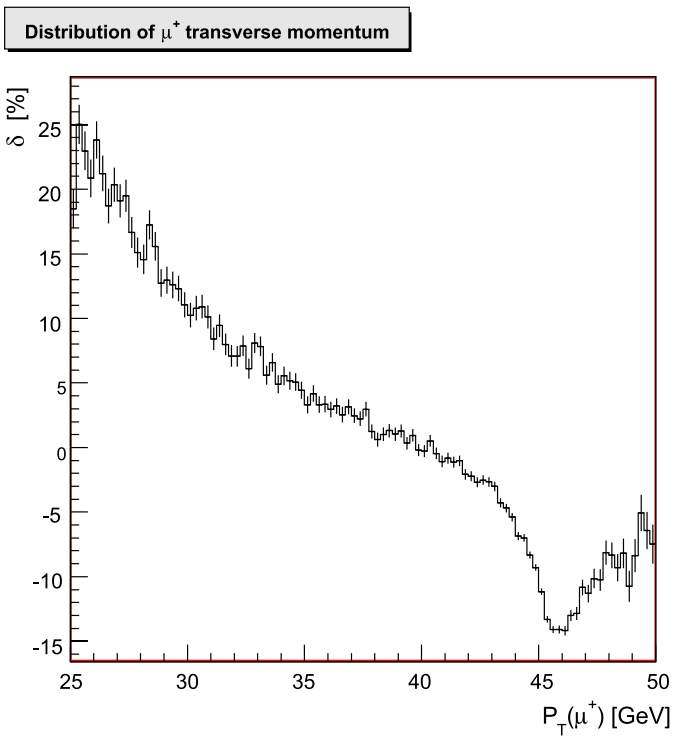

Fig. 5. Relative corrections δ as a function of the muon transverse momentum $p_{\rm T}(\mu^+)$, as obtained from the MC event generator

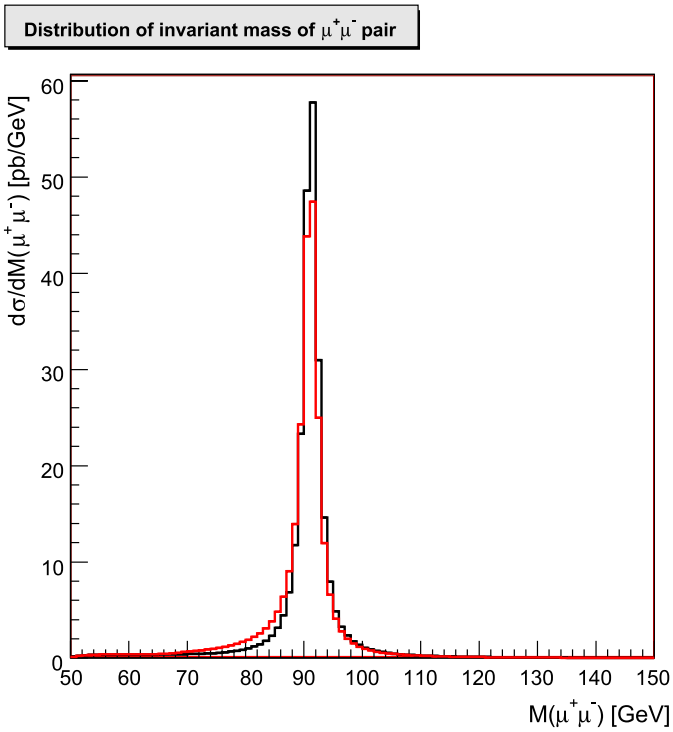

Fig. 6. Invariant mass distribution of the $\mu^+\mu^-$ pair at $\sqrt{s} =$ 14 TeV, as obtained from the MC integrator. Both the Born (*upper line*) and the one-loop results (*lower line*) are shown

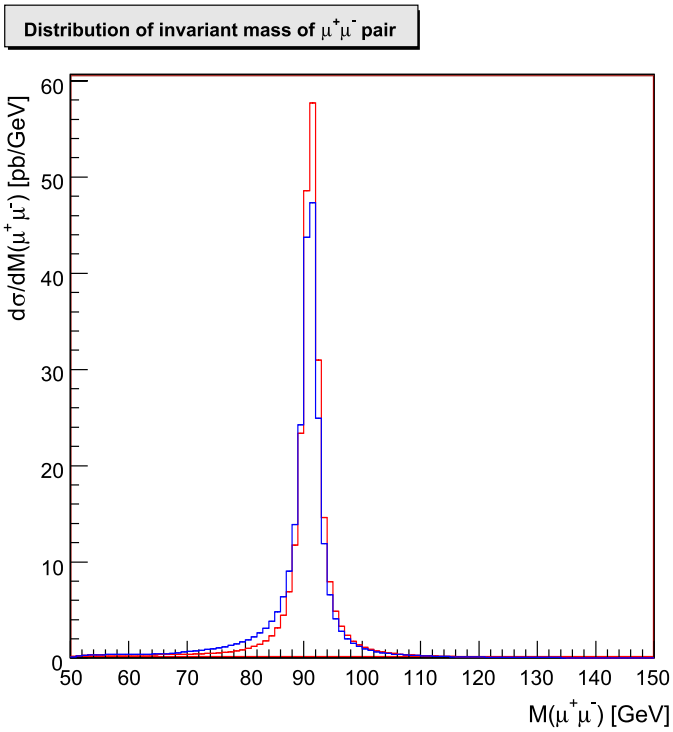

Fig. 8. Invariant mass distribution of the $\mu^+\mu^-$ pair at $\sqrt{s} =$ 14 TeV, as obtained from the MC event generator. Both the Born (*upper line*) and the one-loop results (*lower line*) are shown

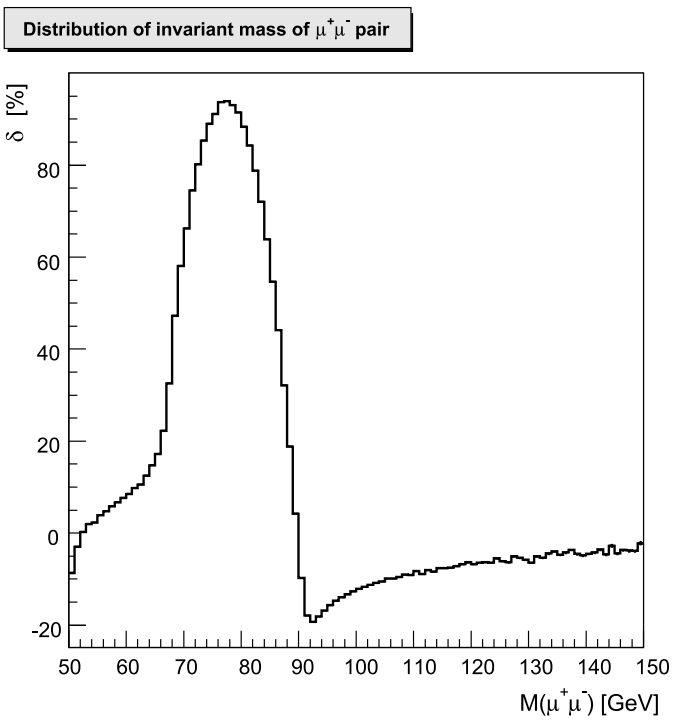

Fig. 7. Relative corrections δ as a function of the invariant mass $M_{\mu^+\mu^-}$, as obtained from the MC integrator

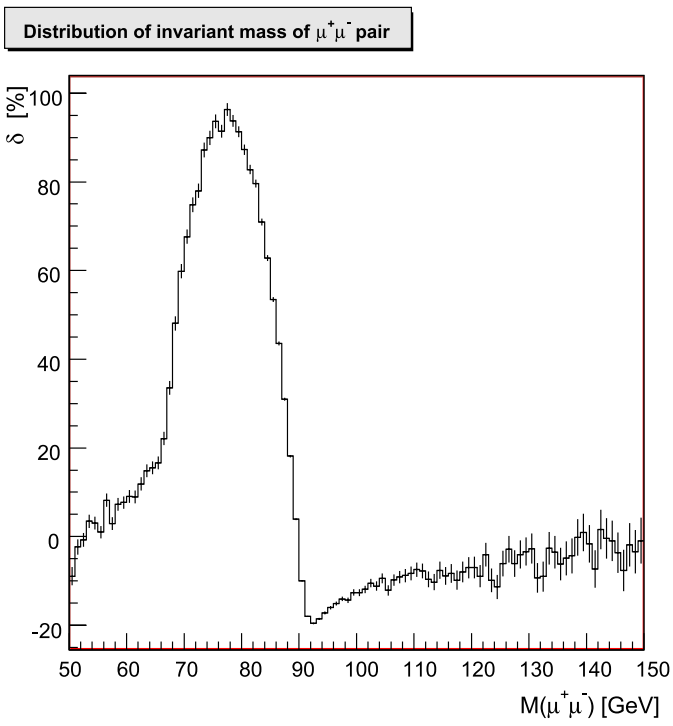

Fig. 9. Relative corrections δ as a function of the invariant mass $M_{\mu^+\mu^-}$, as obtained from the MC event generator

In Figs. 2 and 3 we show the distributions $\mathrm{d}\sigma/\mathrm{d}p_\mathrm{T}$ and $\mathrm{d}\delta/\mathrm{d}p_\mathrm{T}$ obtained with the aid of the MC integrator, while in Figs. 4 and 5 the same distributions were obtained with the aid of the generator. The corresponding distributions agree with each other within the statistical errors, which are larger for the case of the MC event generator.

In Figs. 6 and 7 we show the distributions $\mathrm{d}\sigma/\mathrm{d}M$ and $\mathrm{d}\delta/\mathrm{d}M$ over the invariant mass $M = M_{\mu^+\mu^-}$ for the case of the MC integrator, and in Figs. 8 and 9 for the case of the generator.

One may draw the same conclusions as for the distributions in p_{T}.

Similar distributions are presented in [17], calculated, however, with different setup and cuts; therefore they cannot be compared straightforwardly.

5 Conclusions

In addition to the results presented here, one has to take into account one more $\mathcal{O}(\alpha)$ contribution of the photon-induced subprocess $\gamma + q \to q + l + \bar{l}$, which was recently computed in [38].

In this way the complete set of one-loop electroweak radiative corrections to the neutral current Drell–Yan processes has been computed within the SANC system environment. Our results are implemented into semi-analytical FORTRAN codes as well as into a Monte Carlo event generator. The codes can help to increase the accuracy of the theoretical description of the SM processes, which is required for the forthcoming LHC data analysis. A tuned comparison of our results for NC DY with the ones of analogous calculations performed by other groups, started for the CC case in [21, 22], is in progress within the Les Houches 2007 workshop. The comparison should help us to derive common conclusions on the resulting theoretical uncertainty in our predictions.

Appendix

In the appendix we present a Technical Description of the `sanc_nc_v1.01` package intended for calculation of the total DY NC cross section at the partonic level.

The main aim of this description is to demonstrate how SANC Standard FORTRAN Modules (SSFM) can be used by other codes. We also give a short guide to the main flags that are being used not only in this package but also governing the work of any package that uses SSFM, as our integrators and generators do.

• Overview of the package

All files are produced by the s2n package of the SANC project (v.1.10), except the main*_xx_yy.F, the declaration files, *.h, and the libraries, *.a. Here "xx" and "yy" stand for the standard SANC field indices: $12 - e^-, 13 - u$, $14 - d, 16 - \mu^-$, etc. The package `sanc_dy_nc_v1.00` is accessible for the following set of particles: 1313_1212, 1313_1616, 1414_1212, 1414_1616.

The total set of files inside the package is as follows.

Instruction files:

```
README
RELEASE-NOTES
CHANGES
LICENSE.TXT
INSTALL
```

Declaration files:

```
s2n_declare.h
```

Initialization and various input files:

```
s2n_init.f
sanc_input.h
leshw_input.h
tev4lhcw_input.h
```

Libraries for various functions, including Vegas integration, see INSTALL file in the package.

Main files: `main_nc_vegas_xx_yy.F`

SSFM originating from

```
nc_ff_xx_yy.F  (FF)
nc_si_xx_yy.f  (HA)
nc_br_xx_yy.f  (BR)
[this file contains three SSFM (subroutines)
nc_bo_xx_yy (...), nc_br_xx_yy (...),
nc_ha_xx_xx_1spr (...)]
nc_ha_xx_yy.f  (MC)
```

The steps of the calculation in the `main*` files in accordance with (22), (18), (15) are

- step of declaration and initialization;
- step born is realized by flag iborn=1,
  $\hat{\sigma}_0$ is computed by integration over $\hat{c}$ of (13) of the function_1c_xx_yy,
  - via SSFM call nc_br_xx_yy (...,born,...)
- step $\hat{\sigma}_{\mathrm{SV}}$ is realized by flag iborn=0,
  it is computed by integration over $\hat{c}$ of the function_1c_xx_yy,
  - `virt` via SSFM call nc_si_xx_yy (...,sigma) , (inside this module there exists a call to SSFM nc_ff_xx_yy (...))
  - `soft` via SSFM call nc_br_xx_yy (...,soft,...)
- step $\Delta\hat{\sigma}_{\mathrm{SV}}^{\overline{\mathrm{MS}}}$
  by calculation of $\Delta\hat{\sigma}_{\mathrm{SV}}^{\overline{\mathrm{MS}}}$ through (19)
- step $\Delta\hat{\sigma}_{\mathrm{hard}}^{\overline{\mathrm{MS}}}$
  by integration over ξ of the function_1s_xx_yy
  - via SSFM call nc_bo_xx_yy (...,bornk), see (20)
- step $\mathrm{d}\hat{\sigma}_{\mathrm{hard}}/\mathrm{d}\hat{s}'$
  by integration over $\hat{s}'$ of the function_1spr_xx_yy
  - via SSFM call nc_ha_xx_yy_1spr (...,hard)

  or alternatively
- step $d\sigma_{\mathrm{hard}}/\mathrm{d}\Phi^{(3)}$
  by integration over 4D-phase space of (6)–(7) of the function_4d_xx_yy
  - via SSFM call nc_ha_xx_yy (...,hard).

• Options of the flags

iqed(I) choice of calculations for QED correction:
- $I = 0$ without QED correction;
- $I = 1$ with all QED correction;
- $I = 2$ with ISR QED correction;
- $I = 3$ with IFI QED correction;
- $I = 4$ with FSR QED correction;

iew(I) choice of calculations for EW correction:
$I = 0$ without EW correction;
$I = 1$ with EW correction;

iborn(I) choice of scheme of calculations of the partonic cross section:
$I = 1$ only Born level;
$I = 0$ Born + 1-loop virtual corrections;

gfscheme(I) choice of the EW scheme:
$I = 0$ $\alpha(0)$scheme;
$I = 1$ G_{F} scheme;
$I = 2$ $G_{\mathrm{F}}^{'}$ scheme;

ilin(I) choice of the linearization at the calculation of the partonic cross section:
$I = 0$ without linearization;
$I = 1$ with linearization, i.e. neglecting spurious terms $\mathcal{O}(\alpha^2)$;

ifgg(I) choice of calculations of photonic vacuum polarization $\mathcal{F}_{gg}$:
$I = -1$ — 0;
$I = 0$ — 1;
$I = 1$ — $1 + k\mathcal{F}_{gg}$;
$I = 2$ — $1/(1 - k\mathcal{F}_{gg})$;

with $k = \dfrac{g^2}{16\pi^2}$.

ihard(I) types of the hard bremsstrahlung phase-space integrations:
$I = 1$ integration over $\hat{s}'$;
$I = 4$ 4D integration;

isetup(I) choice of the setup:
$I = 0$ Standard SANC;
$I = 1$ Les Houches Workshop;
$I = 2$ TeV4LHC Workshop.

The package can be accessed from the project homepages [34, 35]

Acknowledgements. We are grateful to V. Kolesnikov, E. Uglov and V. Zykunov for discussions.

This work is partly supported by INTAS Grant Number 03-51-4007, by the EU grant mTkd-CT-2004-510126 in partnership with the CERN Physics Department and by the Polish Ministry of Scientific Research and Information Technology Grant Number 620/E-77/6.PRUE/ DIE 188/2005-2008 and by Russian Foundation for Basic Research Grant Number 07-02-00932. One of us (A.A.) also thanks for the grant of the President RF Scientific Schools 5332.2006.

References

1. S.D. Drell, T.-M. Yan, Phys. Rev. Lett. **25**, 316 (1970)
2. U. Baur, submitted to Int. J. Mod. Phys. E (2007) hep-ph/0701164
3. C.M. Carloni Calame, G. Montagna, O. Nicrosini, F. Piccinini, A. Vicini, AIP Conf. Proc. **870**, 436 (2006)
4. M. Dittmar, F. Pauss, D. Zurcher, Phys. Rev. D **56**, 7284 (1997) [hep-ex/9705004]
5. S. Frixione, M.L. Mangano, JHEP **05**, 056 (2004) [hep-ph/0405130]
6. CDF Collaboration, V.M. Abazov et al., Phys. Rev. D **70**, 092 008 (2004) [hep-ex/0311039]
7. CDF Collaboration, A. Abulencia et al., hep-ex/0508029
8. V.A. Mosolov, N.M. Shumeiko, Nucl. Phys. B **186**, 397 (1981)
9. A.V. Soroko, N.M. Shumeiko, Sov. J. Nucl. Phys. **52**, 329 (1990)
10. D. Wackeroth, W. Hollik, Phys. Rev. D **55**, 6788 (1997) [hep-ph/9606398]
11. U. Baur, S. Keller, D. Wackeroth, Phys. Rev. D **59**, 013 002 (1999) [hep-ph/9807417]
12. S. Dittmaier, M. Kramer, Phys. Rev. D **65**, 073 007 (2002) [hep-ph/0109062]
13. U. Baur, O. Brein, W. Hollik, C. Schappacher, D. Wackeroth, Phys. Rev. D **65**, 033 007 (2002) [hep-ph/0108274]
14. U. Baur, D. Wackeroth, Nucl. Phys. Proc. Suppl. **116**, 159 (2003) [hep-ph/0211089]
15. U. Baur, D. Wackeroth, Phys. Rev. D **70**, 073015 (2004) [hep-ph/0405191]
16. C.M. Carloni Calame, G. Montagna, O. Nicrosini, A. Vicini, JHEP **12**, 016 (2006) [hep-ph/0609170]
17. C.M. Carloni Calame, G. Montagna, O. Nicrosini, A. Vicini, JHEP **10**, 109 (2007) [arXiv:hep-ph/0710.1722]
18. R. Hamberg, W.L. van Neerven, T. Matsuura, Nucl. Phys. B **359**, 343 (1991)
19. C. Anastasiou, L.J. Dixon, K. Melnikov, F. Petriello, Phys. Rev. D **69**, 094 008 (2004) [hep-ph/0312266]
20. K. Melnikov, F. Petriello, Phys. Rev. D **74**, 114 017 (2006) [hep-ph/0609070]
21. C. Buttar et al., hep-ph/0604120
22. TeV4LHC-Top and Electroweak Working Group Collaboration, C.E. Gerber et al., arXiv:hep-ph/0705.3251
23. A. Andonov et al., Comput. Phys. Commun. **174**, 481 (2006) [hep-ph/0411186]
24. A. Andonov et al., Comput. Phys. Commun. **177**, 623 (2007)
25. D. Bardin et al., Comput. Phys. Commun. DOI 10.1016/j.cpc.2007.06.006, hep-ph/0506120
26. C.M. Carloni Calame, G. Montagna, O. Nicrosini, M. Treccani, JHEP **05**, 019 (2005) [hep-ph/0502218]
27. V.A. Zykunov, Phys. Rev. D **75**, 073 019 (2007) [hep-ph/0509315]
28. A. Arbuzov et al., Eur. Phys. J. C **46**, 407 (2006) [hep-ph/0506110]
29. A. Arbuzov et al., Eur. Phys. J. C **50**, 505 (2007)
30. V. Kolesnikov, talk to ATLAS MC, CERN (12, 2006) http://indico.cern.ch/conferenceDisplay.py? confId=6818
31. A. Andonov et al., Phys. Part. Nucl. **4**, 451 (2007) [hep-ph/0610268]
32. S. Jadach, P. Sawicki, Comput. Phys. Commun. **177**, 441 (2007) [physics/0506084]
33. R. Sadykov, talk at ATLAS, CERN (10, 2007) http://indico.cern.ch/conferenceDisplay.py? confId=10887
34. http://sanc.jinr.ru
35. http://pcphsanc.cern.ch
36. W. Hollik, H.J. Timme, Z. Phys. C **33**, 125 (1986)
37. G.P. Lepage, J. Comput. Phys. **27**, 192 (1978)
38. A.B. Arbuzov, R.R. Sadykov, arXiv:hep-ph/0707.0423